

## Study on the HDDR Characteristics of $\text{Nd}_{16}\text{Fe}_{76-x}\text{B}_8\text{Zr}_x$ ( $x = 0-2.0$ ) Alloys and the Magnetic Properties of the HDDR Materials

H. W. Kwon

*Department of Materials Science and Engineering,  
Pukyong National University, Pusan, South Korea, 608-737*

(Received 18 December 1996)

Alloys with compositions based on  $\text{Nd}_{16}\text{Fe}_{76-x}\text{B}_8\text{Zr}_x$  (where  $x = 0-2.0$ ) have been studied to see the effect of Zr addition on HDDR characteristics. A particular emphasis was placed upon the anisotropy of the HDDR material. Anisotropy of the HDDR powder material has been evaluated by comparing the remanence values of the aligned sample measured along the aligning direction and the direction perpendicular to it. The HDDR characteristics of the alloys were investigated by means of DTA and TPA. Magnetic characterisation of the HDDR processed materials was performed using a VSM and a TMA. The magnetic domain structure of the HDDR materials was examined by means of polarised microscope using a solid HDDR processed material. It has been found that small addition (0.1 at %) of Zr to Nd-Fe-B-type alloy retards the disproportionation kinetics of the hydrogenated material. Desorption characteristic of the disproportionated materials has been found not to be affected significantly by the Zr addition. The Zr addition has been found to facilitate the recombination reaction. The intrinsic coercivity of the HDDR powder has been found to depend strongly on the particle size of the powder. As the particle size decreases, the intrinsic coercivity decreases radically, and this is explained in terms of structural damage and/or oxidation caused during mechanical milling. It has also been found that the degree of alignment representing the anisotropic character of the HDDR powder is enhanced with decreasing particle size.

### 1. Introduction

It is well known that Nd-Fe-B-type cast material can be converted into a highly coercive powder by means of the HDDR (hydrogenation, disproportionation, desorption, recombination) process [1]-[3]. The high coercivity of the HDDR powder is believed to be attributed to the recombined fine grain size (typical grain size :  $\sim 0.3 \mu\text{m}$ ) of the material. The HDDR material produced from standard Nd-Fe-B alloy usually shows isotropic behaviour, and this is because the recombined fine crystals exhibit a random orientation without any correlation with the crystal orientation of their parent grain. The isotropic HDDR material, therefore, can not be aligned in a magnetic field, thus not applicable for the production of anisotropic magnets. Fortunately, it has been found that substitutions, such as Zr, Ga, or Hf, for Fe in the Nd-Fe-Co-B-type materials can change the recombination behaviour such that the recombined fine crystals keep their orientation parallel to that of their parent grain. Thus, the HDDR material produced from this type of alloy exhibits anisotropic character [4]-[6]. The induced anisotropy caused by the addition of substituting elements was also observed in the Co-free Nd-Fe-B-type alloys [7]. The HDDR processed anisotropic powder can, therefore, be used

for the production of resin-bonded anisotropic magnets.

In this article, alloys with compositions based on  $\text{Nd}_{16}\text{Fe}_{76-x}\text{B}_8\text{Zr}_x$  (where  $x = 0-2.0$ ) have been studied to see the effect of alloy composition on the HDDR characteristics and the magnetic properties of the HDDR processed materials. We have also examined the variations of intrinsic coercivity and anisotropy of the HDDR processed  $\text{Nd}_{16}\text{Fe}_{75.9}\text{B}_8\text{Zr}_{0.1}$  powder as a function of particle size.

### 2. Experiments

Cast alloys with chemical compositions of  $\text{Nd}_{16}\text{Fe}_{76-x}\text{B}_8\text{Zr}_x$  ( $x = 0-2.0$ ) were prepared using an induction furnace. The cast alloys were annealed at 1000 °C for 2 days under argon gas. DTA (differential thermal analysis) and TPA (thermopiezic analysis) were carried out for the annealed alloys (crushed particles) under hydrogen gas with heating rate of 5 °C/min. The annealed alloy was roughly crushed (around  $5 \times 5 \times 5 \text{ mm}^3$ ), and then subjected to a HDDR process. The crushed pieces were placed into a HDDR system, which was evacuated to a vacuum around  $6 \times 10^{-2}$  mbar. Hydrogen was then introduced into the system to decrepitate the material, and after holding the material at room temperature for 45 mins, the ma-

material was heated at 15 °C/min to the disproportionation temperature (810 °C), and held for the chosen time (2 hrs). The system was then evacuated while maintaining the temperature at 810 °C, and the vacuum allowed to recover. As soon as the vacuum reached a steady value, the furnace was rolled away from the reaction tube containing the material, to avoid unnecessary grain growth of the HDDR processed material. The HDDR processed material was crushed gently using a mortar and pestle or a ball milling. The particle size of the crushed coarse powder and the ball milled fine powder was determined using a standard sieve and a SEM, respectively. Magnetic properties of the HDDR powder were characterised by means of VSM measurements using an aligned sample. The magnetically aligned sample was prepared by setting the green powder in wax in an applied field of 15 kOe. Anisotropy of the HDDR powder was evaluated by using a degree of alignment in the aligned sample, which was defined by the equation given below. In this definition remanence values measured along the aligning direction and the direction perpendicular to it (hereafter transverse direction unless stated otherwise) were used.

$$\text{Degree of alignment (DoA)} = [B_r(P) - B_r(T)] / B_r(P)$$

$B_r(P)$  : remanence along the aligning direction

$B_r(T)$  : remanence along the direction perpendicular to the aligning direction

### 3. Results and Discussion

Annealed alloys were subjected to DTA under hydrogen gas in order to see the reaction between alloy and hydrogen gas, and some DTA traces for the alloys with (0.1 at %) or without Zr are presented in Fig. 1. The traces are featured with two exothermic peaks at lower temperature around 100 °C and at higher temperature at around 700 °C. The exothermic peak appeared at lower temperature may correspond to hydrogenation, which accompanies a massive dissipation of heat, and the exothermic peak at higher temperature to the disproportionation of the hydrogenated material. The disproportionation temperatures of the alloys with different contents of Zr determined by the DTA are tabulated in Table I. The disproportionation temperature was determined by the temperature at which the disproportionation takes place most rapidly. For the Zr-containing alloys the disproportionation was featured with the double peaks. The precise reason for the appearance of the double peaks is not understood well, and the disproportionation temperature was determined by the same way. It is notable that small addition (0.1 at %) of Zr raises the disproportionation temperature by around 20 °C. Further increase in the amount of Zr-addition (more than 0.5 at %), however, seems to reduce slightly the disproportionation temperature of the alloys. This result indicates that the small addition of Zr to the alloy may retard the disproportionation kinetics of the hydrogenated ma-

terial under hydrogen gas.

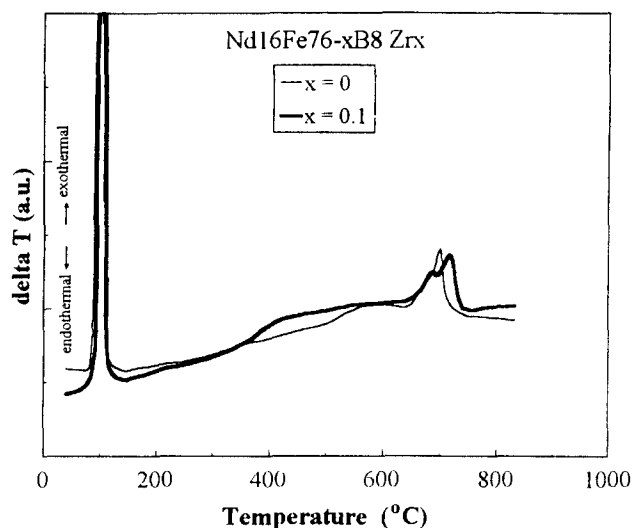


Fig. 1. DTA traces for the alloys with different content of Zr under hydrogen gas.

Table I. Disproportionation temperatures of the  $\text{Nd}_{16}\text{Fe}_{76-x}\text{B}_8\text{Zr}_x$  alloys

Zr content (x)	disproportionation temperature (°C)
0	700
0.1	717
0.5	685
1.0	682
2.0	676

In an attempt to investigate in more detail the effect of Zr addition on the disproportionation kinetics of the hydrogenated material, isothermal TPA tracing on the hydrogenated material was performed at elevated temperatures. Some of the isothermal TPA traces are shown in Fig. 2. Crushed alloys with (0.1 at %) or without Zr were placed into TPA system and the alloys were hydrogenated at 150 °C for 2 hrs, and then the material was allowed to cool down to room temperature. In the meantime, the furnace in the TPA system was heated up to required disproportionation temperature of 700 °C or 800 °C. Sample tube containing the hydrogenated material was brought rapidly into the furnace maintained at the required disproportionation temperature. After bringing the sample tube into the furnace, pressure change was monitored as a function of time.

As can be seen in Fig. 2, the pressure in the sample tube decreases rapidly as the time goes on, and this decrease in pressure is, of course, due to the hydrogen absorption associated with the disproportionation. Of particular note in this result is that the pressure drop due to disproportionation at the temperatures investigated in this study is much slower for the Zr-containing alloy than for the Zr-free alloy. This result indicates that small addition of Zr to the Nd-Fe-B-type alloy may retard

the disproportionation kinetics of the hydrogenated material, and this observation is consistent with the result observed from the DTA (Fig. 1). It can also be found that at higher temperature around 800 °C, the hydrogenated material is disproportionated very rapidly. It seems that most of the disproportionation is accomplished within around 5 minutes. Fig. 3 shows the TMA traces for the materials disproportionated very briefly. The materials used for these TMA traces were fully hydrogenated and disproportionated at 800 °C for 5 minutes under hydrogen gas and then quenched very rapidly. The TMA traces of the briefly disproportionated materials show that the materials have magnetic phase(s) with Curie temperature above the range of the present study. This magnetic phase with high Curie temperature may be  $\alpha$ -Fe which is formed as a result of the disproportionation. Little evidence of the presence of nondisproportionated  $Nd_2Fe_{14}BH_4$  phase can be found in these briefly disproportionated materials. This result means that most of the disproportionation reaction of

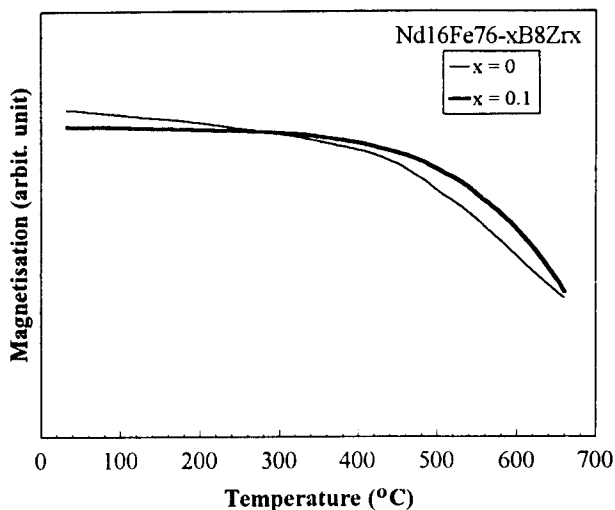
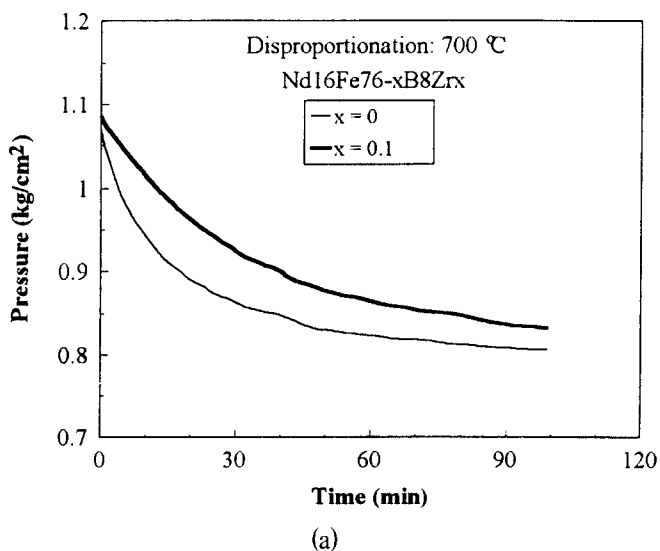


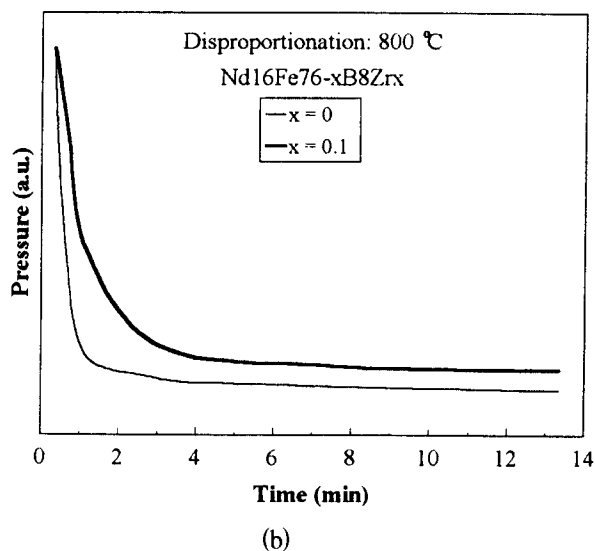
Fig. 3. TMA traces for the materials disproportionated very briefly. The materials were fully hydrogenated and disproportionated at 800 °C for 5 minutes under hydrogen gas and then quenched very rapidly.

the hydrogenated material is accomplished in the very early stage at high temperature (800 °C).

The desorption characteristics of the disproportionated material at elevated temperature under vacuum were examined using an isothermal TPA. Materials disproportionated at 800 °C for 2 hours were cooled quickly down to 700 °C. (Desorption at temperature higher than 700 °C was taking place too rapidly, and it was not appropriate to examine the desorption characteristic.) After arriving at the temperature, TPA system containing the materials was evacuated. Pressure change in the sample tube during the evacuation was monitored as a function of evacuating time at the temperature, and the results are shown in Fig. 4. It appears that the pressure drop during the desorption



(a)



(b)

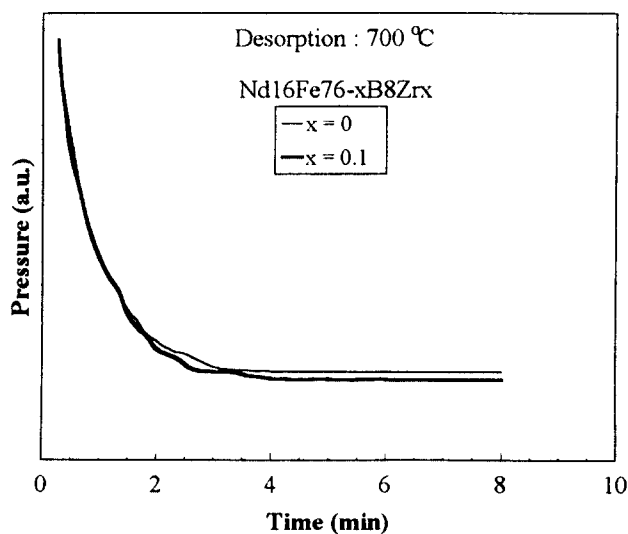


Fig. 4. Isothermal TPA traces for the disproportionated materials showing desorption characteristics.

Fig. 2. Isothermal TPA traces on the hydrogenated material at elevated temperature under hydrogen gas.

is exactly the same for the alloys with or without Zr, and most of the desorption is completed in the very early stage of the evacuation (within 4 minutes). These results lead us to conclude that the desorption characteristics of the disproportionated material may not be affected significantly by the Zr-addition.

The recombination characteristic of the disproportionated materials with different contents of Zr was studied by measuring the intrinsic coercivity of the very briefly recombined materials. The materials were fully hydrogenated (at 150 °C for 2 hrs under 1 bar hydrogen gas) and disproportionated. As soon as the disproportionation was completed, the system was evacuated using rotary vacuum pump, and, at the same time, the furnace was pulled out to cool rapidly the material. This treatment leads to a very brief desorption and recombination, and the recombination takes place just during cooling. The 2nd quadrant demagnetisation curves for these materials are shown in Fig. 5. It appears that the intrinsic coercivity of the HDDR materials from the alloy with 2 at % Zr (around 8.5 kOe) is much higher than that of the material from the Zr-free alloy (around 3 kOe). The intrinsic coercivity of the briefly recombined materials with different Zr-content are tabulated in Table II. The higher intrinsic coercivity of the material with higher Zr-content indicates that a greater degree of recombination has been achieved for the materials with higher Zr. This result leads us to conclude that the Zr addition may facilitate the recombination.

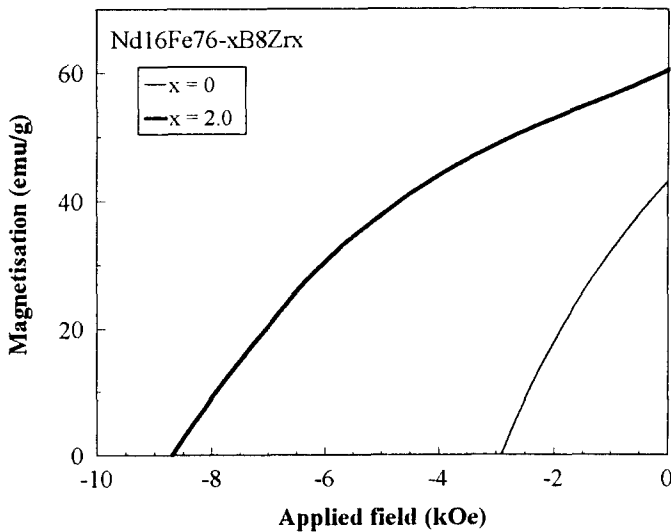


Fig. 5. Demagnetisation curves of the very briefly recombined materials.

Table II. Intrinsic coercivity of the briefly recombined  $\text{Nd}_{16}\text{Fe}_{76-x}\text{B}_8\text{Zr}_x$  materials.

x	intrinsic coercivity (kOe)
0	3.0
0.1	4.3
1.0	5.7
2.0	8.5

Fig. 6 shows Kerr image observed from fully or partially HDDR processed materials. The HDDR materials processed through a conventional route usually have a very friable character. The materials conventionally HDDR processed, therefore, can not be used for observing the microstructure and magnetic domain structure. In the present study, in order to prepare a solid sample adequate for a structural observation, a variation of conventional HDDR process, which is called a solid HDDR process [8] was employed. The partially processed sample was prepared using very brief hydrogenation and disproportionation. After the introduction of hydrogen at 650 °C into the system, the sample was heated rapidly toward the disproportionation temperature, 810 °C. As soon as the sample temperature reached the disproportionation temperature, the system was evacuated to start the desorption and recombination. Meanwhile, the fully processed sample was prepared through the usual solid HDDR process (disproportionation at 810 °C for 2 hrs, desorption and recombination at 810 °C for 1 hr). The microstructure and magnetic domain structure of the HDDR samples were observed by an optical microscope using a polarised light, and the results are shown in Fig. 6. Also included in Fig. 6 is the magnetic domain structure of the bulk alloy before HDDR process for comparison. The Kerr image of bulk alloy before the HDDR shows a coarse grain size and a clear magnetic domain structure of each grain. The microstructure of the partially processed sample reveals that only the regions near the boundary between the  $\text{Nd}_2\text{Fe}_{14}\text{B}$  grain and the Nd-rich phase region have been HDDR processed and the interior of the grain remains intact. Magnetic domain structure of the recombined region can not be observed in the micrograph, and this is simply because the recombined crystals are too fine to be observed by optical microscope. It can also be found that the HDDR reactions initiated from the region near the boundary between the  $\text{Nd}_2\text{Fe}_{14}\text{B}$  grain and the Nd-rich phase and then proceeded toward the interior of each grain. This result would seem to indicate that the Nd-rich grain boundary phase may play an important role in the HDDR process. The Nd-rich phase may act as an effective path for diffusion of hydrogen atom. The Kerr image of the fully HDDR processed sample appears to have no magnetic domain structure. In this sample whole grain has actually been well HDDR processed, and the recombined grains in each parent grain are so fine that the size of the recombined crystal may be comparable to the critical single domain size of the  $\text{Nd}_2\text{Fe}_{14}\text{B}$  compound (around 0.3  $\mu\text{m}$ ). Although the recombined crystals may actually have magnetic domain structure, it is virtually impossible to see the very fine domain structure under the optical microscope with poor resolution.

The 2nd quadrant demagnetization characteristics of the HDDR material produced from the  $\text{Nd}_{16}\text{Fe}_{75.9}\text{B}_8\text{Zr}_{0.1}$  alloy immediately after the HDDR treatment (lightly crushed) were measured along the two different directions in the VSM using an aligned and bonded sample, and the result is presented in

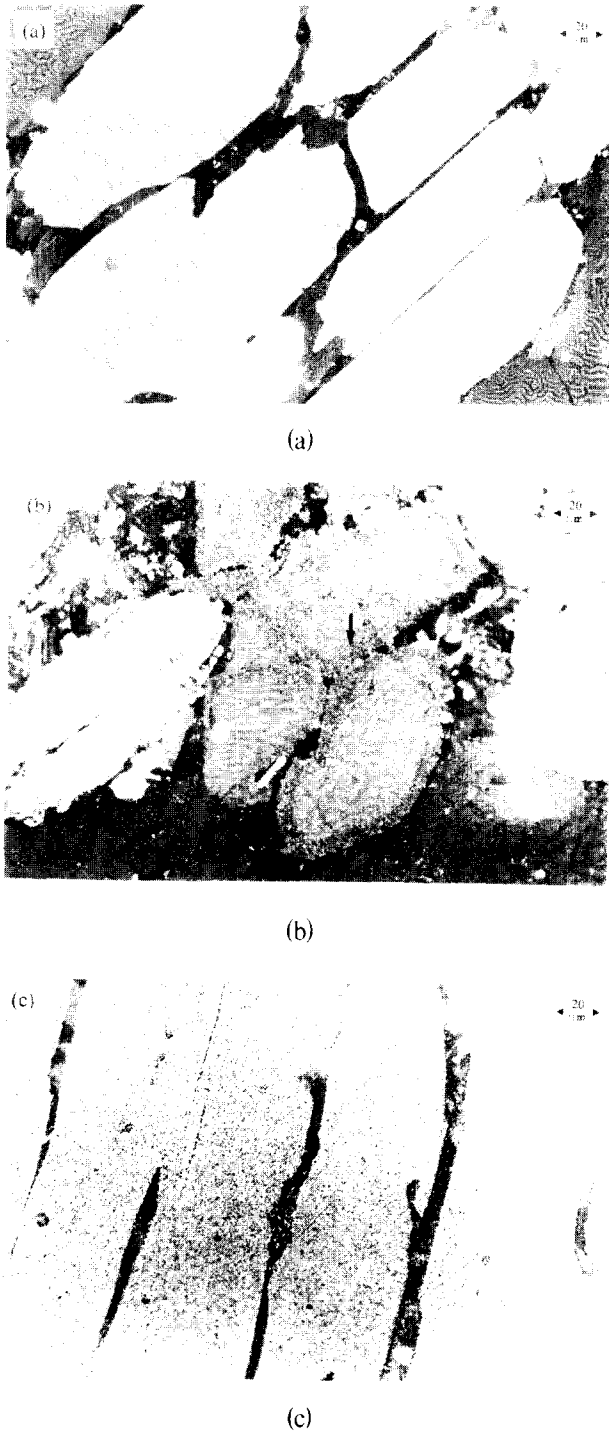


Fig. 6. Kerr image micrographs showing the microstructure and magnetic domain structure of materials at various conditions. (a) before HDDR, (b) partially HDDR processed (arrow indicates the HDDR treated region), (c) fully HDDR processed.

Fig. 7. As can be seen, the intrinsic coercivity of the material is appreciable (over 12 kOe), and the high coercivity of HDDR processed materials may be attributed to the fine recombined grain size. The same alloy showed very low intrinsic coercivity (less than 1 kOe) before the HDDR treatment. It appears that the demagnetization curves measured along the aligning direction or transverse direction show exactly the same demagnetis-

ation characteristics. Of particular note in this result is that the remanence values along the aligning or the transverse direction exhibits virtually no difference between them. This would suggest that there is no anisotropic character in this HDDR material produced from  $Nd_{16}Fe_{75.9}B_8Zr_{0.1}$  alloy. It has been reported that HDDR material obtained from Zr-containing Nd-Fe-B-type materials usually exhibits a considerable anisotropy [7]. Considering this fact, the present result is somewhat surprising. Also included in the Fig. 7 is the demagnetization curves obtained along different directions for the same HDDR material after ball milling for 15 hrs (average particle size : around  $7 \mu m$ ). It is found that the intrinsic coercivity of the milled powder is reduced radically to less than 6 kOe, which is half the value before milling, and the remanence values measured along the two different directions are now significantly different. The remanence along the aligning direction exhibits a much higher value with respect to that along the transverse direction. The marked reduction in the coercivity can be attributed to structural damage and/or oxidation during milling. The difference in remanence values can be attributed to a significant degree of anisotropy in this powder. This result indicates that the HDDR material produced from the  $Nd_{16}Fe_{75.9}B_8Zr_{0.1}$  alloy is magnetically anisotropic. It is also found from this result that the HDDR material which is magnetically anisotropic in nature can show isotropic character depending upon the particle size. It should be noted, therefore, that a correct evaluation of the anisotropic character of HDDR materials requires to use powder with appropriate particle size.

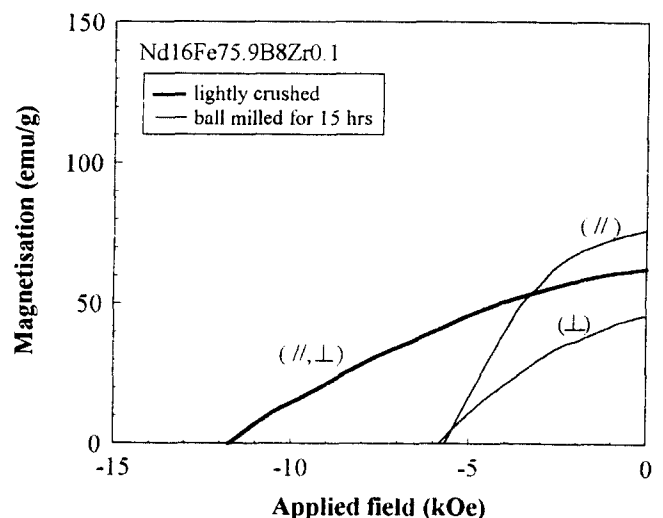


Fig. 7. Demagnetization curves measured along different directions for HDDR treated  $Nd_{16}Fe_{75.9}B_8Zr_{0.1}$  material with different particle size.

The above findings have shown that the intrinsic coercivity and the anisotropic characteristics of the HDDR material may vary with the particle size. Variations of the intrinsic coercivity and the degree of alignment, which represents anisotropic

character, of the HDDR processed  $\text{Nd}_{16}\text{Fe}_{75.9}\text{B}_8\text{Zr}_{0.1}$  material as a function of particle size of the powder have been investigated, and the results are shown in Fig. 8. It appears that the intrinsic coercivity of HDDR material decreases radically with decreasing particle size. This observation can be attributed to the structural damage and/or oxidation caused during milling, as discussed above. This might pose a serious challenge to the production of useful HDDR powder material with high coercivity for application as resin-bonded anisotropic magnet. Meanwhile, the degree of alignment, which represents the degree of anisotropy of the powder material, appears to increase gradually with decreasing particle size. This variation can probably be explained by noting that coarser particles are more likely to consist of a large number of recombined fine grains which come from different parent grains (see Fig. 9). These coarser particles may, then, exhibit smaller degree of anisotropy even though each parent grain has been recombined into a fine grained structure in an anisotropic manner. As the particle size decreases, however, it is more likely for a particle to consist of fine recombined grains those come from a common parent grain (see Fig. 9). The powder with finer particle size will then exhibit more anisotropic character.

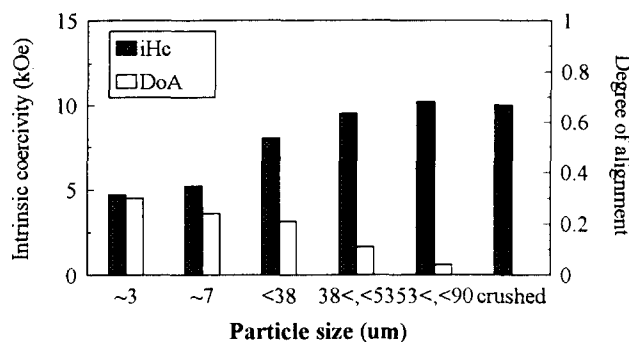


Fig. 8. Variations of intrinsic coercivity and degree of alignment of HDDR processed  $\text{Nd}_{16}\text{Fe}_{75.9}\text{B}_8\text{Zr}_{0.1}$  material as a function of particle size. Particle size of the lightly crushed powder was around 120 μm.

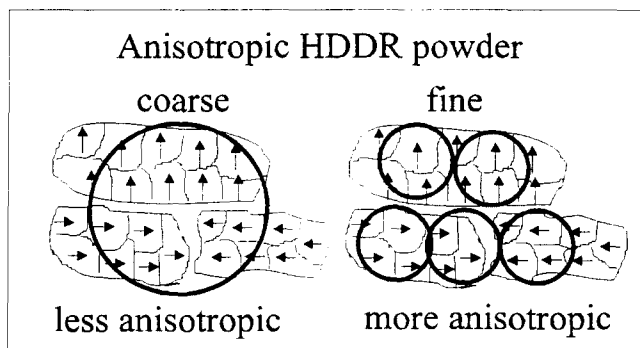


Fig. 9. Schematic illustration showing anisotropy of anisotropic HDDR material with different particle size. The easy magnetisation directions of the neighboring recombined grains may, in fact, not be perfectly parallel to each other.

It should be interesting to compare the degree of anisotropy of the HDDR material with that of a commercial Nd-Fe-B-type anisotropic sintered magnet. For this comparison, the  $\text{Nd}_{16}\text{Fe}_{75.9}\text{B}_8\text{Zr}_{0.1}$  HDDR material produced under optimum condition and the commercial anisotropic sintered magnet (RES-270) from Philips Components (UK) were used. The HDDR material were ball milled for 24 hrs, and the prepared fine powder (average particle size : around 3 μm) was aligned in magnetic field and bonded, and then subjected to the VSM measurement. For evaluating the degree of anisotropic character of the commercial anisotropic magnet, a small block ( $3 \times 3 \times 3 \text{ mm}^3$ ) was cut from the sintered magnet. Demagnetisation curves of the bonded HDDR sample and the sintered block were measured along the two different directions, and the results are shown in Fig. 10. The degrees of alignment for the HDDR material and the sintered block are calculated to be around 0.5 and around 0.7, respectively. It appears that the anisotropic character of the HDDR material processed in optimum condition in the present study is lower significantly with respect to the commercial sintered magnet.

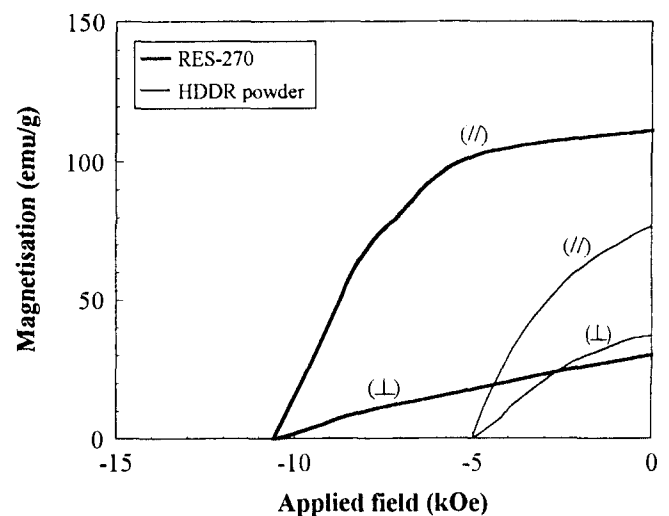


Fig. 10. Comparison of the degree of anisotropic character between HDDR material and commercial sintered anisotropic magnet.

### Conclusion

Alloys with compositions based on  $\text{Nd}_{16}\text{Fe}_{76-x}\text{B}_8\text{Zr}_x$  (where  $x = 0-2.0$ ) have been studied to see the effect of alloy composition on the HDDR characteristics and the magnetic properties of the HDDR processed materials. It has been found that the small addition (0.1 at %) of Zr was found to retard the disproportionation kinetics of the hydrogenated material. Desorption characteristic of the disproportionated materials was not affected significantly by the Zr addition. The Zr addition was found to facilitate the recombination reaction of the disproportionated material. The intrinsic coercivity of the HDDR powder was found to depend strongly on the particle

size of the powder. As the particle size decreases, the intrinsic coercivity decreases radically, and this result is interpreted in terms of structural damage and/or oxidation in the particle caused during mechanical milling. The degree of alignment representing the degree of anisotropic character of the HDDR powder was found to be improved with decreasing particle size.

### Acknowledgment

This work was supported by the Korean Ministry of Education (Grant for research on advanced materials in 1995).

### References

- [1] T. Takeshita and R. Nakayama, *Proceedings of 10th Int. Workshop on RE Magnets and Their Applications*, Kyoto, Japan, 551 (1989).
- [2] I. R. Harris, *Proceedings of 12th Int. Workshop on RE Magnets and Their Applications*, Canberra, Australia, 347 (1992).
- [3] D. Book and I. R. Harris, *IEEE Trans. Magn.*, **MAG-28**, 2145 (1992).
- [4] P. J. McGuinness, X. J. Zhang, H. Forsyth, and I. R. Harris, *J. Less-Common Metals*, **162**, 379 (1991).
- [5] T. Takeshita and R. Nakayama, *Proceedings of 11th Int. Workshop on RE Magnets and Their Applications*, Pittsburgh, USA, 49 (1990).
- [6] T. Takeshita and R. Nakayama, *Proceedings of 12th Int. Workshop on RE Magnets and Their Applications*, Canberra, Australia, 670 (1992).
- [7] P. J. McGuinness, C. J. Short, and I. R. Harris, *IEEE Trans. Magn.*, **MAG-29**, 2145 (1993).
- [8] X. J. Zhang, P. J. McGuinness, and I. R. Harris, *J. Appl. Phys.*, **69**, 5838 (1991).